

Article

Pulsed Broad-Spectrum UV Light Effectively Inactivates SARS-CoV-2 on Multiple Surfaces and N95 Material

Alexander S. Jureka , Caroline G. Williams  and Christopher F. Basler * 

Center for Microbial Pathogenesis, Institute for Biomedical Sciences, Georgia State University, Atlanta, GA 30303, USA; ajureka@gsu.edu (A.S.J.); cwilliams334@student.gsu.edu (C.G.W.)

* Correspondence: cbasler@gsu.edu; Tel.: +1-(404)-413-3651

Abstract: The ongoing SARS-CoV-2 pandemic has resulted in an increased need for technologies capable of efficiently disinfecting public spaces as well as personal protective equipment. UV light disinfection is a well-established method for inactivating respiratory viruses. Here, we have determined that broad-spectrum, pulsed UV light is effective at inactivating SARS-CoV-2 on multiple surfaces in vitro. For hard, non-porous surfaces, we observed that SARS-CoV-2 was inactivated to undetectable levels on plastic and glass with a UV dose of 34.9 mJ/cm² and stainless steel with a dose of 52.5 mJ/cm². We also observed that broad-spectrum, pulsed UV light is effective at reducing SARS-CoV-2 on N95 respirator material to undetectable levels with a dose of 103 mJ/cm². We included UV dosimeter cards that provide a colorimetric readout of UV dose and demonstrated their utility as a means to confirm desired levels of exposure were reached. Together, the results presented here demonstrate that broad-spectrum, pulsed UV light is an effective technology for the in vitro inactivation of SARS-CoV-2 on multiple surfaces.



Citation: Jureka, A.S.; Williams, C.G.; Basler, C.F. Pulsed Broad-Spectrum UV Light Effectively Inactivates SARS-CoV-2 on Multiple Surfaces and N95 Material. *Viruses* **2021**, *13*, 460. <https://doi.org/10.3390/v13030460>

Academic Editor:
Luis Martinez-Sobrido

Received: 14 February 2021
Accepted: 9 March 2021
Published: 11 March 2021

Publisher's Note: MDPI stays neutral with regard to jurisdictional claims in published maps and institutional affiliations.



Copyright: © 2021 by the authors. Licensee MDPI, Basel, Switzerland. This article is an open access article distributed under the terms and conditions of the Creative Commons Attribution (CC BY) license (<https://creativecommons.org/licenses/by/4.0/>).

Keywords: ultraviolet; SARS-CoV-2; COVID-19; coronavirus; inactivation

1. Introduction

In late 2019, the novel severe acute respiratory distress syndrome coronavirus 2 (SARS-CoV-2) was first reported in Wuhan, China [1,2]. SARS-CoV-2 is a member of the *Coronaviridae* family of enveloped negative-sense RNA viruses. It is classified in the *Betacoronavirus* genus of which other notable members are the highly pathogenic SARS-CoV and the Middle East respiratory syndrome virus (MERS-CoV) [3]. Since its emergence, SARS-CoV-2 has been the cause of the most severe pandemic in the last century. Despite significant efforts to contain the spread of SARS-CoV-2, as of February 7th, 2021, it has caused over 105 million cases and resulted in over 2.3 million deaths worldwide [4].

High case counts raise concerns about infections arising from contaminated public spaces, such as mass transit vehicles and hospital spaces that have housed SARS-CoV-2-positive patients. The need for effective means to eliminate SARS-CoV-2 from environmental surfaces is supported by studies demonstrating the capacity of the virus to survive on a variety of surfaces for significant periods of time. For example, infectious virus could be recovered from plastic or steel for 72 h and on cardboard after 24 h [5]. There is also substantial evidence that SARS-CoV-2-infected individuals shed virus into their environment. Analysis by RT-PCR of COVID-19 patient rooms and other hospital settings demonstrated frequent contaminating viral RNA on surfaces [6–9]. In some studies, however, a lower frequency of surface contamination has been reported [10]. Outside of the healthcare setting, rooms of cruise ship passengers who had COVID-19 were also contaminated with viral RNA [11]. Viral RNA has also been found on various surfaces in households with SARS-CoV-2 infected individuals [12,13].

Given the potential for fomite transmission, the World Health Organization has provided guidance on cleaning and disinfection where SARS-CoV-2 contamination could occur [14]. Due to the importance of respiratory protection and shortages of personal

protective equipment, methods to disinfect and reuse N95 filtering respirators have also been of significant interest [15,16]. UV light as well as other methods have been either proposed or tested as a means to disinfect N95 masks and other personal protective equipment (PPE) [16–24].

While chemical disinfectants and alcohols are effective methods of inactivating SARS-CoV-2 in most circumstances, disinfection of large spaces using these methods is a laborious process requiring close contact with potentially contaminated surfaces [25–28]. UV light has long been established as an effective and direct method for the inactivation of enveloped viruses [29]. UV disinfection approaches provide a significant advantage as they are less laborious to employ and do not necessarily require close contact with potentially contaminated surfaces. The UV spectrum is divided into three sub-spectra: UV-A (315–400 nm), UV-B (280–315 nm), and UV-C (100–280 nm). Most current studies that have focused on the efficacy of UV light in inactivating SARS-CoV-2 utilize devices that produce solely UV-C light [28,30–33]. UV-C light is the most common UV sub-spectra produced by commercially available UV disinfection devices due to its well-known germicidal properties [34]. UV devices producing broad-spectrum UV light (consisting of UV-A, -B, -C, and visible light) are also available [35]. One possible advantage of the longer UV wavelengths is that they could lower levels of absorption in samples containing organic materials [34].

Here, we report the *in vitro* efficacy of a commercially available UV disinfection device (Helo F2; Puro Lighting) that produces broad-spectrum (200–700 nm), pulsed UV light in inactivating SARS-CoV-2 on glass, plastic, stainless steel, and N95 respirator material. Additionally, we have tested the efficacy of UV dosimeter cards that would provide end users the ability to quickly determine if a high enough dosage of UV light has been applied to a surface. Together, the data reported here demonstrate that broad-spectrum, pulsed UV light is highly effective at inactivating SARS-CoV-2 on multiple surfaces.

2. Materials and Methods

2.1. Cells and Virus

Vero E6 cells (ATCC# CRL-1586) were maintained in DMEM supplemented with heat-inactivated fetal bovine serum (FBS; Gibco, Waltham, MA, USA). SARS-CoV-2, isolate USA_WA1/2020, was obtained from the World Reference Collection for Emerging Viruses and Arboviruses at the University of Texas Medical Branch. SARS-CoV-2 virus stocks were propagated as previously described [36].

2.2. Surface and N95 Material Inoculation

The following surfaces were tested within the wells of a 24 well plate in triplicate: glass coverslips, 0.5 × 0.5 cm stainless steel squares, the tissue culture plate well (plastic; polystyrene), and 0.5 × 0.5 cm squares of N95 respirator material from a 3M™ 9210+ respirator. Four 0.5 × 0.5 cm squares of UV dosimeter cards (Intelligo Technologies, Stockholm, Sweden) were placed in each corner of the plate to confirm even UV exposure across the plates and allow comparison of the cards to a UV dosage meter as a means to quantify exposure dose (Supplemental Figure S1). For surface inoculation, 12 µL of SARS-CoV-2 stock virus (USA_WA1/2020; 8.3×10^4 pfu) in OptiMEM supplemented with 1 × antibiotic/antimycotic (Gibco, Waltham, MA, USA) was pipetted directly onto each surface being tested and spread with a pipette tip to facilitate efficient drying. Surface and N95 material samples inoculated with virus were allowed to dry in the 24 well plates with lids off for 1 h at room temperature in the biosafety cabinet. After the surfaces had dried, the 24-well plate lids were replaced, and all plates not being exposed to UV were placed inside a black opaque container in a separate biosafety cabinet to avoid incidental UV exposure.

2.3. UV Exposures

The Helo F2 device (Puro Lighting, Lakewood, CO, USA) is a self-contained pulsed UV device that consists of two high energy xenon lamps that produce broad-spectrum UV

light (200–700 nm). Upon activation, the device produces a 2 ms pulse every 6 s until the pre-set duty cycle is completed (≤ 30 min), the built-in motion detector is triggered, or power is disconnected from the device.

The Helo F2 device was placed in the center of the biosafety cabinet. The test samples as well as a UV dosage meter (ILT2500; International Light Technologies, Peabody, MA, USA) equipped with a calibrated SED270 detector were placed 1 m away facing the Helo F2 device. Care was taken to ensure that the UV dosage meter and surfaces being exposed were as inline as possible before beginning testing. The 24-well plates containing the test surfaces were positioned so that the plates were nearly vertical (~ 85 degrees) and approximately 3 inches above the surface of the biosafety cabinet to avoid shadowing (Supplemental Figure S2). Once the 24-well plate was positioned, the UV dosage meter was zeroed to account for ambient UV. Once zeroed, the UV dosage meter was set to “integrate” mode to measure UV dosage over time and total pulse-counts. The Helo F2 device was initiated using an electronic timer set to the indicated exposure time with an additional minute added to account for device startup procedures. UV dosage for a given timepoint was recorded as mJ/cm^2 along with the corresponding pulse-count. UV dosimeter cards were collected and photographed to record the color change. One card from the 3-min timepoint was lost due to airflow in the biosafety cabinet. For the purposes of graphical depiction, UV dosimeter card color post-UV exposure was replicated using the eyedropper tool in Adobe Illustrator. Determination of the correlation between the Helo F2 pulse counts and dosage was performed by plotting the data on the X and Y axis, respectively, and fitting the data with a linear regression in GraphPad Prism (GraphPad Software, San Diego, CA, USA; Version 9).

2.4. Sample Harvesting

After all exposures were complete, 1 mL of sterile PBS was placed inside the surface- and N95 material-containing wells and was allowed to rehydrate for 15 min before transferring to a 1.5 mL centrifuge tube and storing at -80 °C for further analysis. Additionally, 12 μL containing 8.3×10^4 pfu of stock virus (USA_WA1/2020) was added to 1 mL of sterile PBS and stored at -80 °C at the same time as the other samples in order to control for the loss of virus titer due to the drying process.

2.5. Virus Quantification by Plaque Assay

Vero E6 cells were plated to confluency in 24-well plates 24 h prior to infection. Ten-fold serial dilutions of SARS-CoV-2-containing samples were added onto the cells (100 μL) and virus was adsorbed for 1 h with shaking at 15-min intervals. After the adsorption period, 1 mL of 0.6% microcrystalline cellulose in DMEM supplemented with 2% fetal bovine serum and $1 \times$ antibiotic-antimycotic was overlaid onto the cells and plates were incubated at 37 C/ 5% CO_2 for 72 h, as described previously [36]. After incubation, the microcrystalline cellulose overlay was aspirated from the well, and cells were fixed with 10% neutral buffered formalin for 1 h at room temperature. Plates were then washed with water and stained with crystal violet to visualize plaques. Plaques were quantified and recorded as plaque-forming units per mL (pfu/mL). All samples assayed were only subjected to one freeze–thaw cycle.

3. Results

3.1. Correlation of UV Dosage and Pulse Counts

We first determined the range of UV dosage that could be achieved with the Helo F2 device between 1 and 30 min of exposure. The device produces a theoretical 10 pulses per minute. In practice, we achieved 6 pulses after 1 min and 297 pulses after 30 min, corresponding to cumulative UV doses of 3.14 and 103 mJ/cm^2 , respectively (Figure 1A,B). Interestingly, we observed the UV dosage output by the Helo F2 device over time has a significant and linear correlation with the overall pulse count (Figure 1C). This suggests that it is possible to identify a specific amount of time required for inactivation depending

on the dosage required. Additionally, the exposure times and UV dosage range tested in this study encompass previously reported effective UV exposure times and doses for inactivating SARS-CoV-2 with other commercially available UV devices [33,35].

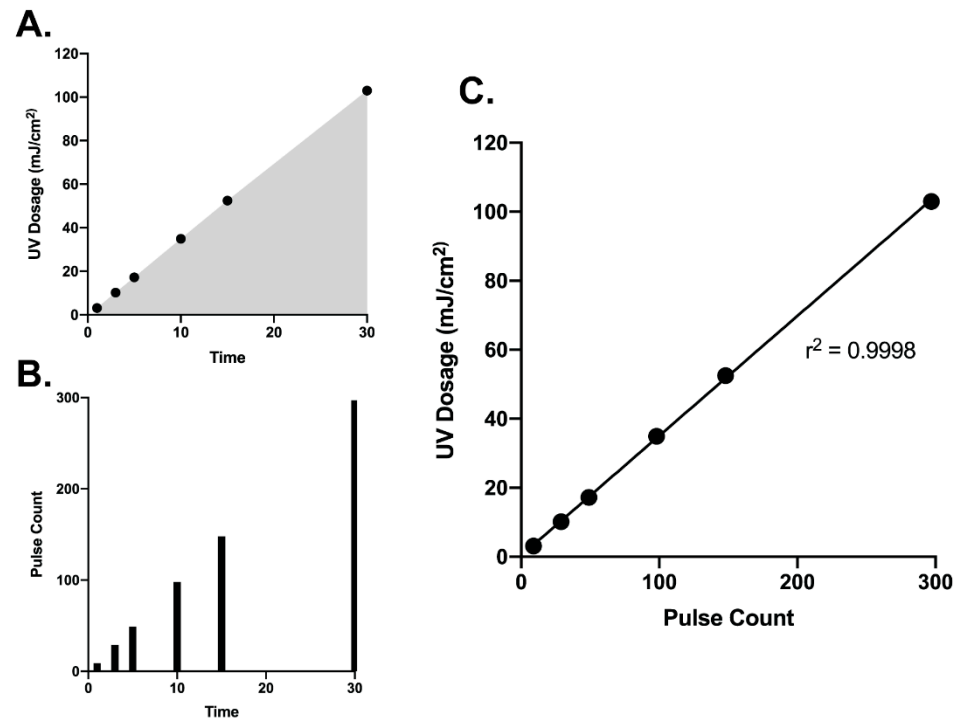


Figure 1. UV dosage (A) and pulse counts (B) recorded over time from the Helo F2 device. (C) Pulse count plotted versus UV dosage shows a significant positive correlation. Data were fit with a linear regression in GraphPad prism.

3.2. Broad Spectrum Pulsed UV Light Effectively Inactivates SARS-CoV-2 On Multiple Surfaces and N95 Material

To determine the efficacy of the Helo F2 device in inactivating SARS-CoV-2, glass, stainless steel, plastic, and N95 respirator material inoculated with SARS-CoV-2 (see materials and methods) were exposed to pulsed UV light for 1, 3, 5, 10, 15, and 30 min from a distance of 1 m. Time zero represents samples that were inoculated, dried and quantified for infectivity without UV exposure. SARS-CoV-2 titers recovered from the unexposed UV controls indicate that the drying process resulted in an approximately 3-fold decrease in titers when compared to the same inoculum that had not been dried prior to titration (Figure 2). Additionally, similar amounts of SARS-CoV-2 were recovered from all surfaces, indicating that the recovery process was efficient for all tested surfaces.

For the UV-exposed samples, we observed that for the hard, non-porous surfaces (glass, stainless steel, and plastic), a pulse-on time of 5 min (17.2 mJ/cm²) was sufficient to achieve a 3-log₁₀ reduction in infectious virus recovered from the surfaces (Figure 3A–C). Exposure for 10 min (34.9 mJ/cm²) was sufficient to reduce infectious virus to nearly undetectable levels on glass and plastic, while 15 min (52.5 mJ/cm²) was required for the same effect on stainless steel. N95 respirator material (3M 9210+) required 15 min of exposure to achieve a 2.86 log₁₀ reduction in infectious virus and 30 min (103 mJ/cm²) exposure for reduction to undetectable levels, which is likely due to the porous and multilayer structure of N95 material (Figure 3D) [32,37,38]. Taken together, these data suggest that broad-spectrum pulsed UV light produced by the Helo F2 is capable of effectively inactivating SARS-CoV-2 in short periods of time on hard, non-porous surfaces, and on N95 respirator material with longer exposure times.

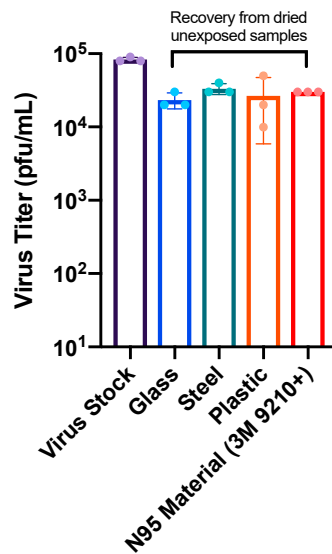


Figure 2. Virus titer reduction due to drying. Virus stock represents the amount of virus initially inoculated onto the surfaces. Glass, steel, plastic, and 3M N95 material samples represent the virus titer recovered from dried, unexposed samples after harvesting.

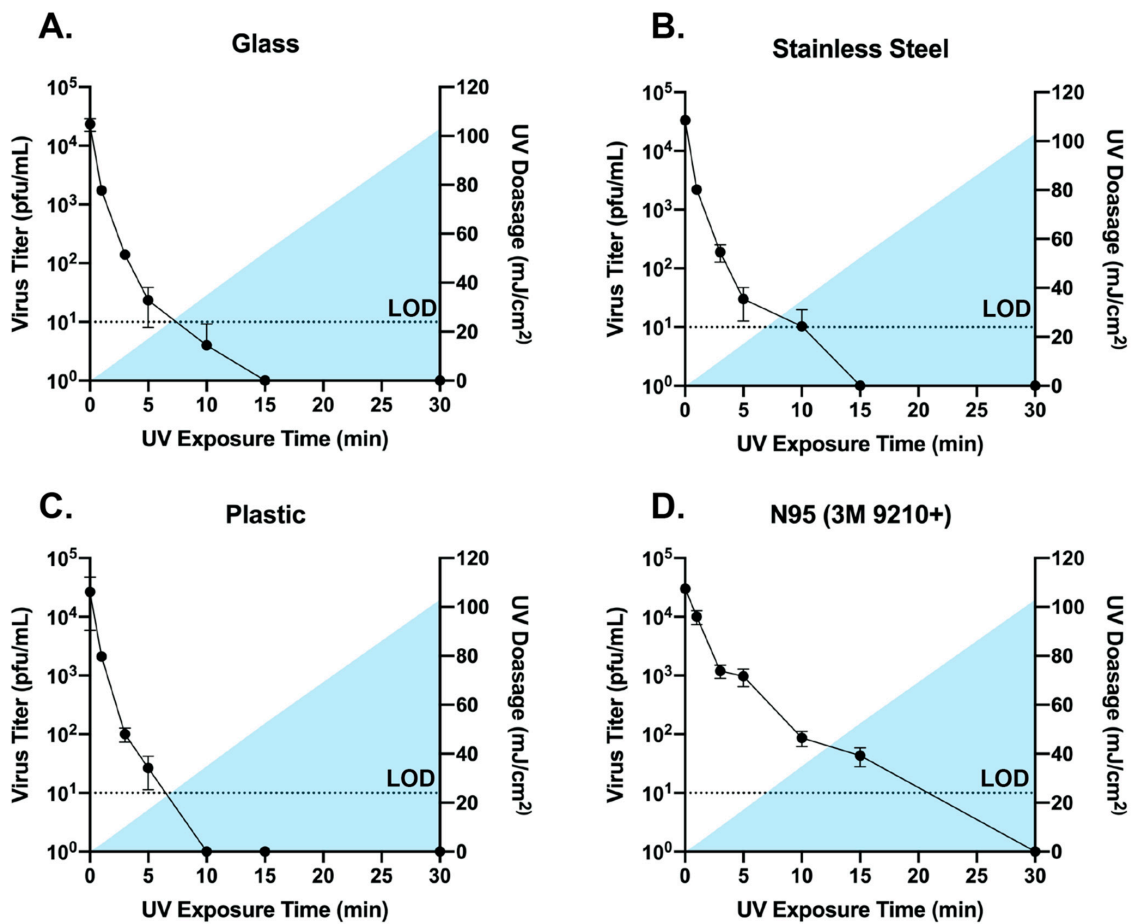


Figure 3. Titers of infectious SARS-CoV-2 recovered from UV-exposed glass, stainless steel, plastic, and N95 material (A–D). Time 0 represents controls that were not exposed to UV. All timepoints are representative of the mean and standard error of 3 replicates. Blue shading represents the area under the curve for the UV dosage acquired over time. Samples with data points below the limit of detection (LOD, dotted line; 10 pfu) resulted from a subset of datapoints having undetectable levels of virus. Undetected samples were assigned a value of 1 for graphing purposes.

3.3. Correlating Colorimetric UV Dosimeter Cards to Physical UV Dosimeter and Virus Titer Reductions

In tandem with testing the effectiveness of broad-spectrum UV light in inactivating SARS-CoV-2, we also evaluated the functionality of UV dosage cards specifically designed for pulsed UV light sources. To test their functionality, four test pieces of experimental UV dosage card material were included in each UV exposure timepoint. We determined that these functioned as intended with a significant color change occurring with increasing doses of UV (Figure 4A). We identified that the color change was even across all cards recovered at each timepoint, indicating a high degree of reproducibility across the material (Supplemental Figure S3). We compiled our UV dosage meter and SARS-CoV-2 titer reduction data to correlate with the color change from the cards (Figure 4B). Taken together, this UV-reactive card material represents an accurate alternative to high-cost photodiode-based UV dosimeters for end users of broad-spectrum pulsed UV disinfection equipment.

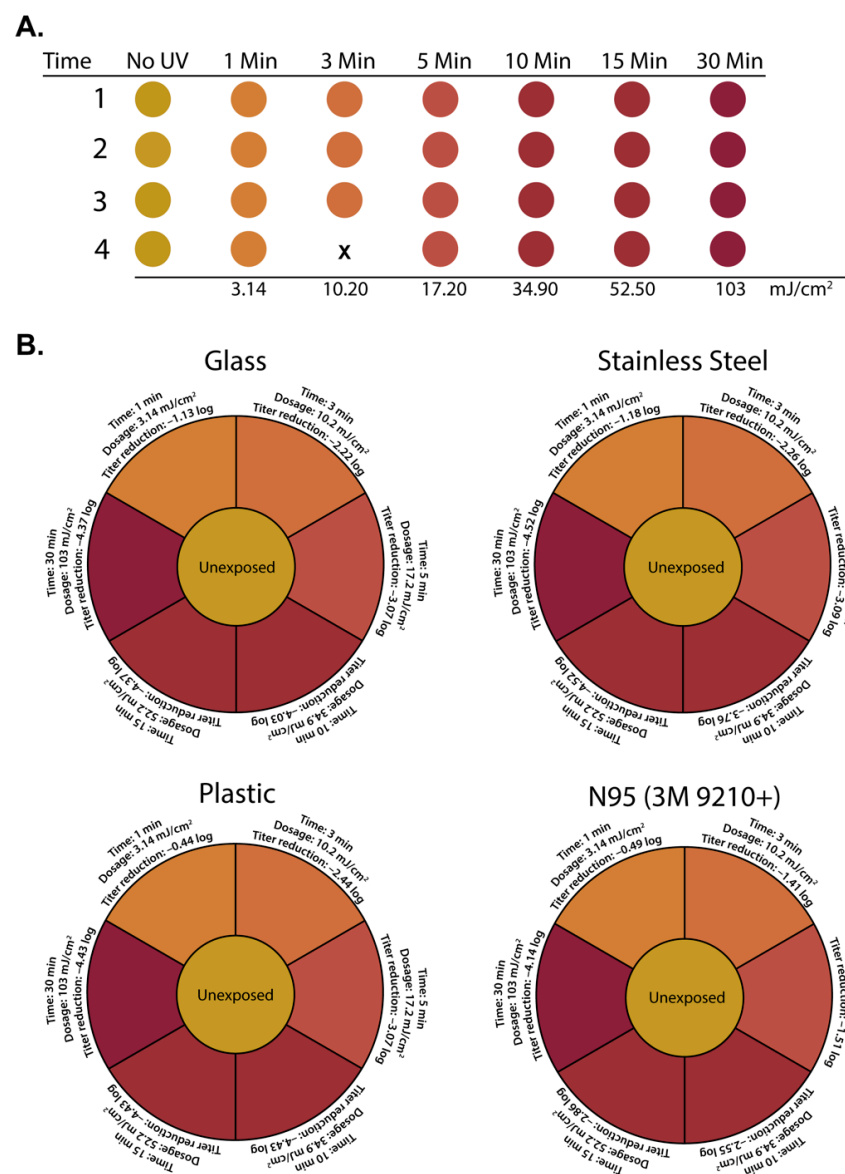


Figure 4. (A) Colorimetric change of indicator cards at indicated timepoints and dosages. (B) Compilation of time, dosage, and SARS-CoV-2 titer reduction data as a function of indicator card color. Indicator color in (A,B) is graphically depicted by using the eyedropper color tool within Adobe Illustrator on recovered UV indicator cards.

4. Discussion

The availability of information regarding the inactivation of SARS-CoV-2 for environmental disinfection is of paramount importance. UV disinfection is a validated technology that has been utilized for decades to inactivate pathogens on surfaces, as well as in air and water [39,40]. The effectiveness of UV light, pulsed or constant, in inactivating pathogens is expected to be directly related to the dosage and wavelengths applied [37]. Here, we have described empirically determined dosages of broad-spectrum, pulsed UV light output by the Helo F2 device that are effective for the inactivation of SARS-CoV-2 on multiple relevant surfaces and N95 respirator material. Additionally, we have also demonstrated the effectiveness of colorimetric UV dosimeter cards for dosage determination by the end-user. It should be noted that the UV light emitted by the Helo F2 device is broad-spectrum (200–700 nm) and therefore, would not be safe for use in occupied spaces.

While only a single device was tested in this study, a variety of UV inactivation studies have been published focusing on SARS-CoV-2 and other coronaviruses using different wavelengths and environmental conditions [30,31,41–45]. In contrast to the broad-spectrum UV device tested here, most UV devices that have been tested for efficacy against SARS-CoV-2 produce constant, non-pulsed UV-C (222–300 nm) light exclusively [28,30–33]. One other study has focused on a UV device that produces pulsed UV from high intensity xenon lamps; however, the wavelengths produced by the device were not reported [35]. The efficacy of the device tested in this study was determined based on exposure time as opposed to the UV dose applied to the test surfaces. Our study is the first to report the efficacy of a broad-spectrum, pulsed, UV (200–700 nm) device in terms of both time and the effective UV dose.

Disinfection of potentially contaminated surfaces by UV light is a particularly attractive option when compared to chemical disinfectants as it is less laborious and does not require close contact with contaminated surfaces. Additionally, with PPE shortages being an ongoing concern, our data demonstrate that broad-spectrum pulsed UV should be explored further as a strategy for the disinfection of N95 respirators. This warrants further exploration, as our study only examined one model of mask and did not determine how pulsed UV exposure affects N95 performance. In addition, it will be important to take into account the materials from which a particular mask is made and how it is constructed, because these factors might alter the efficiency with which virus inactivation occurs.

While our data demonstrate that broad-spectrum pulsed UV light is an effective method for inactivating SARS-CoV-2, one notable limitation of our study is that surfaces were only exposed to the UV light at a distance of one meter in a laboratory setting under a single set of environmental conditions. However, our data demonstrated that colorimetric UV dosimeter cards work as expected and provide a clear indication of the dosage being applied to a particular surface where the card is in place. In the event that a surface is more than one meter from a given UV device, using our data as a reference, the inverse square law could be applied to determine the amount of time required to achieve a particular dosage at the necessary distance [46–48].

From a point-of-use perspective, electronic photodiode-based UV dosimeters like the one employed here are expensive and require manual set-up and operation. An alternative would be the use of UV dosimeter cards that exhibit a colorimetric change in response to increasing doses of UV light. Our data demonstrate that such cards provide an accurate readout for UV dose from a broad-spectrum, pulsed, UV device. UV dosimeter cards like those tested here would provide a simple, rapid, and low-cost method for testing broad-spectrum pulsed UV light devices at different distances to ensure that an effective dosage is delivered in a real-world setting.

The data presented here demonstrate that broad-spectrum UV light is an effective means of inactivating SARS-CoV-2 on multiple surfaces and N95 respirator material. Additionally, UV dosimeter cards like those tested here represent an effective and straightforward means for point-of-care users of UV disinfection equipment to ensure that surfaces have been properly disinfected.

Supplementary Materials: The following are available online at <https://www.mdpi.com/1999-4915/13/3/460/s1>, Figure S1: Test plate arrangement, Figure S2: Experimental setup, Figure S3: UV dosimeter cards collected from each test plate.

Author Contributions: A.S.J. and C.F.B. designed the experiments. A.S.J. and C.G.W. performed the experiments. A.S.J. and C.F.B. wrote the manuscript. All authors have read and agreed to the published version of the manuscript.

Funding: Funds for these studies were provided by Puro UV Disinfection Lighting.

Institutional Review Board Statement: Not Applicable.

Informed Consent Statement: Not Applicable.

Data Availability Statement: The data in this manuscript will be made available upon request from the corresponding author.

Acknowledgments: We would like to acknowledge the GSU High Containment Core for their assistance in performing these studies.

Conflicts of Interest: PURO UV Disinfection Lighting provided the Puro UV Helo F2 device, the UV dosimeter cards, the UV meter and funds for the studies described. All data and analyses were collected and performed without input from PURO UV Disinfection Lighting.

References

1. Zhu, N.; Zhang, D.; Wang, W.; Li, X.; Yang, B.; Song, J.; Zhao, X.; Huang, B.; Shi, W.; Lu, R.; et al. A Novel Coronavirus from Patients with Pneumonia in China, 2019. *N. Engl. J. Med.* **2020**, *382*, 727–733. [[CrossRef](#)] [[PubMed](#)]
2. Holshue, M.L.; DeBolt, C.; Lindquist, S.; Lofy, K.H.; Wiesman, J.; Bruce, H.; Spitters, C.; Ericson, K.; Wilkerson, S.; Tural, A.; et al. First Case of 2019 Novel Coronavirus in the United States. *N. Engl. J. Med.* **2020**, *382*, 929–936. [[CrossRef](#)]
3. Gorbalenya, A.E.; Baker, S.C.; Baric, R.S.; de Groot, R.J.; Drosten, C.; Gulyaeva, A.A.; Haagmans, B.L.; Lauber, C.; Leontovich, A.M.; Neuman, B.W.; et al. The species Severe acute respiratory syndrome-related coronavirus: Classifying 2019-nCoV and naming it SARS-CoV-2. *Nat. Microbiol.* **2020**, *5*, 536–544. [[CrossRef](#)]
4. COVID-19 Weekly Epidemiological Update 7 February 2021; World Health Organization: Geneva, Switzerland, 2020.
5. van Doremalen, N.; Bushmaker, T.; Morris, D.H.; Holbrook, M.G.; Gamble, A.; Williamson, B.N.; Tamin, A.; Harcourt, J.L.; Thornburg, N.J.; Gerber, S.I.; et al. Aerosol and Surface Stability of SARS-CoV-2 as Compared with SARS-CoV-1. *N. Engl. J. Med.* **2020**, *382*, 1564–1567. [[CrossRef](#)]
6. Zhou, J.; Otter, J.A.; Price, J.R.; Cimpeanu, C.; Garcia, D.M.; Kinross, J.; Boshier, P.R.; Mason, S.; Bolt, F.; Holmes, A.H.; et al. Investigating SARS-CoV-2 surface and air contamination in an acute healthcare setting during the peak of the COVID-19 pandemic in London. *Clin. Infect. Dis.* **2020**. [[CrossRef](#)]
7. Santarpia, J.L.; Rivera, D.N.; Herrera, V.L.; Morwitzer, M.J.; Creager, H.M.; Santarpia, G.W.; Crown, K.K.; Brett-Major, D.M.; Schnaubelt, E.R.; Broadhurst, M.J.; et al. Aerosol and surface contamination of SARS-CoV-2 observed in quarantine and isolation care. *Sci. Rep.* **2020**, *10*, 12732. [[CrossRef](#)]
8. Ong, S.W.X.; Tan, Y.K.; Chia, P.Y.; Lee, T.H.; Ng, O.T.; Wong, M.S.Y.; Marimuthu, K. Air, Surface Environmental, and Personal Protective Equipment Contamination by Severe Acute Respiratory Syndrome Coronavirus 2 (SARS-CoV-2) From a Symptomatic Patient. *JAMA* **2020**, *323*, 1610–1612. [[CrossRef](#)] [[PubMed](#)]
9. Guo, Z.D.; Wang, Z.Y.; Zhang, S.F.; Li, X.; Li, L.; Li, C.; Cui, Y.; Fu, R.B.; Dong, Y.Z.; Chi, X.Y.; et al. Aerosol and Surface Distribution of Severe Acute Respiratory Syndrome Coronavirus 2 in Hospital Wards, Wuhan, China, 2020. *Emerg. Infect. Dis.* **2020**, *26*, 1583–1591. [[CrossRef](#)] [[PubMed](#)]
10. Colaneri, M.; Seminari, E.; Novati, S.; Asperges, E.; Biscarini, S.; Piralla, A.; Percivalle, E.; Cassaniti, I.; Baldanti, F.; Bruno, R.; et al. Severe acute respiratory syndrome coronavirus 2 RNA contamination of inanimate surfaces and virus viability in a health care emergency unit. *Clin. Microbiol. Infect.* **2020**, *26*, 1094 e1091–1094 e1095. [[CrossRef](#)]
11. Suzuki, M.; Kamiya, H.; Okamoto, K.; Yamagishi, T.; Kakimoto, K.; Takeda, M.; Matsuyama, S.; Shirato, K.; Nao, N.; Hasegawa, H.; et al. Environmental sampling for severe acute respiratory syndrome coronavirus 2 (SARS-CoV-2) during a coronavirus disease (COVID-19) outbreak aboard a commercial cruise ship. *medRxiv* **2020**. [[CrossRef](#)]
12. Maestre, J.P.; Jarra, D.; Yu, C.; Siegel, J.; Horner, S.; Kinney, K.A. Distribution of SARS-CoV-2 RNA Signal in a Home with COVID-19 Positive Occupants. *medRxiv* **2020**. [[CrossRef](#)]
13. Döhla, M.; Wilbring, G.; Schulte, B.; Kümmerer, B.M.; Diegmann, C.; Sib, E.; Richter, E.; Haag, A.; Engelhart, S.; Eis-Hübinger, A.M.; et al. SARS-CoV-2 in environmental samples of quarantined households. *medRxiv* **2020**. [[CrossRef](#)]
14. World Health Organization. *Cleaning and Disinfection of Environmental Surfaces in the Context of COVID-19: Interim Guidance, 15 May 2020*; World Health Organization: Geneva, Switzerland, 2020.
15. Paul, D.; Gupta, A.; Maurya, A.K. Exploring options for reprocessing of N95 Filtering Facepiece Respirators (N95-FFRs) amidst COVID-19 pandemic: A systematic review. *PLoS ONE* **2020**, *15*, e0242474. [[CrossRef](#)]

16. Derraik, J.G.B.; Anderson, W.A.; Connelly, E.A.; Anderson, Y.C. Rapid Review of SARS-CoV-1 and SARS-CoV-2 Viability, Susceptibility to Treatment, and the Disinfection and Reuse of PPE, Particularly Filtering Facepiece Respirators. *Int. J. Environ. Res. Public Health* **2020**, *17*, 6117. [[CrossRef](#)] [[PubMed](#)]
17. Ma, Q.X.; Shan, H.; Zhang, C.M.; Zhang, H.L.; Li, G.M.; Yang, R.M.; Chen, J.M. Decontamination of face masks with steam for mask reuse in fighting the pandemic COVID-19: Experimental supports. *J. Med. Virol.* **2020**, *92*, 1971–1974. [[CrossRef](#)] [[PubMed](#)]
18. Ibanez-Cervantes, G.; Bravata-Alcantara, J.C.; Najera-Cortes, A.S.; Meneses-Cruz, S.; Delgado-Balbuena, L.; Cruz-Cruz, C.; Duran-Manuel, E.M.; Cureno-Diaz, M.A.; Gomez-Zamora, E.; Chavez-Ocana, S.; et al. Disinfection of N95 masks artificially contaminated with SARS-CoV-2 and ESKAPE bacteria using hydrogen peroxide plasma: Impact on the reutilization of disposable devices. *Am. J. Infect. Control* **2020**, *48*, 1037–1041. [[CrossRef](#)] [[PubMed](#)]
19. Hamzavi, I.H.; Lyons, A.B.; Kohli, I.; Narla, S.; Parks-Miller, A.; Gelfand, J.M.; Lim, H.W.; Ozog, D.M. Ultraviolet germicidal irradiation: Possible method for respirator disinfection to facilitate reuse during the COVID-19 pandemic. *J. Am. Acad. Derm.* **2020**, *82*, 1511–1512. [[CrossRef](#)] [[PubMed](#)]
20. Daeschler, S.C.; Manson, N.; Joachim, K.; Chin, A.W.H.; Chan, K.; Chen, P.Z.; Tajdaran, K.; Mirmoeini, K.; Zhang, J.J.; Maynes, J.T.; et al. Effect of moist heat reprocessing of N95 respirators on SARS-CoV-2 inactivation and respirator function. *CMAJ* **2020**, *192*, E1189–E1197. [[CrossRef](#)]
21. Chou, R.; Dana, T.; Jungbauer, R.; Weeks, C.; McDonagh, M.S. Masks for Prevention of Respiratory Virus Infections, Including SARS-CoV-2, in Health Care and Community Settings: A Living Rapid Review. *Ann. Intern. Med.* **2020**, *173*, 542–555. [[CrossRef](#)]
22. Cheng, V.C.C.; Wong, S.C.; Kwan, G.S.W.; Hui, W.T.; Yuen, K.Y. Disinfection of N95 respirators by ionized hydrogen peroxide during pandemic coronavirus disease 2019 (COVID-19) due to SARS-CoV-2. *J. Hosp. Infect.* **2020**, *105*, 358–359. [[CrossRef](#)]
23. Celina, M.C.; Martinez, E.; Omana, M.A.; Sanchez, A.; Wiemann, D.; Tezak, M.; Dargaville, T.R. Extended use of face masks during the COVID-19 pandemic—Thermal conditioning and spray-on surface disinfection. *Polym. Degrad. Stab.* **2020**, *179*, 109251. [[CrossRef](#)] [[PubMed](#)]
24. Carrillo, I.O.; Floyd, A.C.E.; Valverde, C.M.; Tingle, T.N.; Zabaneh, F.R. Immediate-use steam sterilization sterilizes N95 masks without mask damage. *Infect. Control Hosp. Epidemiol.* **2020**, *41*, 1104–1105. [[CrossRef](#)] [[PubMed](#)]
25. Al-Sayah, M.H. Chemical disinfectants of COVID-19: An overview. *J. Water Health* **2020**, *18*, 843–848. [[CrossRef](#)]
26. Kratzel, A.; Todt, D.; V'kovski, P.; Steiner, S.; Gultom, M.L.; Thao, T.T.N.; Ebert, N.; Holwerda, M.; Steinmann, J.; Niemeyer, D.; et al. Efficient inactivation of SARS-CoV-2 by WHO-recommended hand rub formulations and alcohols. *bioRxiv* **2020**. [[CrossRef](#)]
27. Leslie, R.A.; Zhou, S.S.; Macinga, D.R. Inactivation of SARS-CoV-2 by commercially available alcohol-based hand sanitizers. *Am. J. Infect. Control* **2020**. [[CrossRef](#)] [[PubMed](#)]
28. Xiling, G.; Yin, C.; Ling, W.; Xiaosong, W.; Jingjing, F.; Fang, L.; Xiaoyan, Z.; Yiyue, G.; Ying, C.; Lunbiao, C.; et al. In vitro inactivation of SARS-CoV-2 by commonly used disinfection products and methods. *Sci. Rep.* **2021**, *11*, 2418. [[CrossRef](#)]
29. Budowsky, E.I.; Bresler, S.E.; Friedman, E.A.; Zheleznova, N.V. Principles of selective inactivation of viral genome. I. UV-induced inactivation of influenza virus. *Arch. Virol.* **1981**, *68*, 239–247. [[CrossRef](#)] [[PubMed](#)]
30. Biasin, M.; Bianco, A.; Pareschi, G.; Cavalleri, A.; Cavatorta, C.; Fenizia, C.; Galli, P.; Lessio, L.; Lualdi, M.; Tombetti, E.; et al. UV-C irradiation is highly effective in inactivating SARS-CoV-2 replication. *medRxiv* **2021**. [[CrossRef](#)]
31. Buonanno, M.; Welch, D.; Shuryak, I.; Brenner, D.J. Far-UVC light (222 nm) efficiently and safely inactivates airborne human coronaviruses. *Sci. Rep.* **2020**, *10*, 10285. [[CrossRef](#)] [[PubMed](#)]
32. Cadnum, J.L.; Li, D.F.; Redmond, S.N.; John, A.R.; Pearlmutter, B.; Donskey, C.J. Effectiveness of Ultraviolet-C Light and a High-Level Disinfection Cabinet for Decontamination of N95 Respirators. *Pathog. Immun.* **2020**, *5*, 52–67. [[CrossRef](#)]
33. Kitagawa, H.; Nomura, T.; Nazmul, T.; Omori, K.; Shigemoto, N.; Sakaguchi, T.; Ohge, H. Effectiveness of 222-nm ultraviolet light on disinfecting SARS-CoV-2 surface contamination. *Am. J. Infect. Control* **2020**. [[CrossRef](#)] [[PubMed](#)]
34. Hessling, M.; Hones, K.; Vatter, P.; Lingenfelder, C. Ultraviolet irradiation doses for coronavirus inactivation-review and analysis of coronavirus photoinactivation studies. *GMS Hyg. Infect. Control* **2020**, *15*, Doc08. [[CrossRef](#)] [[PubMed](#)]
35. Simmons, S.E.; Carrion, R.; Alfson, K.J.; Staples, H.M.; Jinadatha, C.; Jarvis, W.R.; Sampathkumar, P.; Chemaly, R.F.; Khawaja, F.; Povroznik, M.; et al. Deactivation of SARS-CoV-2 with pulsed-xenon ultraviolet light: Implications for environmental COVID-19 control. *Infect. Control Hosp. Epidemiol.* **2020**. [[CrossRef](#)]
36. Jureka, A.S.; Silvas, J.A.; Basler, C.F. Propagation, Inactivation, and Safety Testing of SARS-CoV-2. *Viruses* **2020**, *12*, 622. [[CrossRef](#)] [[PubMed](#)]
37. Raeiszadeh, M.; Adeli, B. A Critical Review on Ultraviolet Disinfection Systems against COVID-19 Outbreak: Applicability, Validation, and Safety Considerations. *Acs Photonics* **2020**, *7*, 2941–2951. [[CrossRef](#)]
38. Mills, D.; Harnish, D.A.; Lawrence, C.; Sandoval-Powers, M.; Heimbuch, B.K. Ultraviolet germicidal irradiation of influenza-contaminated N95 filtering facepiece respirators. *Am. J. Infect. Control* **2018**, *46*, e49–e55. [[CrossRef](#)]
39. Bolton, J.R.; Cotton, C.A. *The Ultraviolet Disinfection Handbook*, 1st ed.; American Water Works Association: Denver, CO, USA, 2008; pp. 1–9. 149p.
40. Kowalski, W.J. *Ultraviolet Germicidal Irradiation Handbook: UVGI for Air and Surface Disinfection*; Springer: New York, NY, USA, 2009; pp. 1–16. 501p.
41. Pendyala, B.; Patras, A.; Pokharel, B.; D'Souza, D. Genomic Modeling as an Approach to Identify Surrogates for Use in Experimental Validation of SARS-CoV-2 and HuNoV Inactivation by UV-C Treatment. *Front. Microbiol.* **2020**, *11*, 572331. [[CrossRef](#)] [[PubMed](#)]

42. Patterson, E.I.; Prince, T.; Anderson, E.R.; Casas-Sanchez, A.; Smith, S.L.; Cansado-Utrilla, C.; Solomon, T.; Griffiths, M.J.; Acosta-Serrano, A.; Turtle, L.; et al. Methods of Inactivation of SARS-CoV-2 for Downstream Biological Assays. *J. Infect. Dis.* **2020**, *222*, 1462–1467. [[CrossRef](#)] [[PubMed](#)]
43. Inagaki, H.; Saito, A.; Sugiyama, H.; Okabayashi, T.; Fujimoto, S. Rapid inactivation of SARS-CoV-2 with deep-UV LED irradiation. *Emerg. Microbes Infect.* **2020**, *9*, 1744–1747. [[CrossRef](#)]
44. Simmons, S.; Carrion, R.; Alfson, K.; Staples, H.; Jinadatha, C.; Jarvis, W.; Sampathkumar, P.; Chemaly, R.F.; Khawaja, F.; Povroznik, M.; et al. Disinfection effect of pulsed xenon ultraviolet irradiation on SARS-CoV-2 and implications for environmental risk of COVID-19 transmission. *medRxiv* **2020**. [[CrossRef](#)]
45. Shining a light on COVID-19. *Nat. Photonics* **2020**, *14*, 337. [[CrossRef](#)]
46. Bolton, J.R.; Linden, K.G. Standardization of methods for fluence (UV dose) determination in bench-scale UV experiments. *J. Environ. Eng-Asce* **2003**, *129*, 209–215. [[CrossRef](#)]
47. Harrington, B.J.; Valigosky, M. Monitoring ultraviolet lamps in biological safety cabinets with cultures of standard bacterial strains on TSA blood agar. *Labmedicine* **2007**, *38*, 165–168. [[CrossRef](#)]
48. Lin, C.Y.; Li, C.S. Control effectiveness of ultraviolet germicidal irradiation on bioaerosols. *Aerosol. Sci. Tech.* **2002**, *36*, 474–478. [[CrossRef](#)]